Log in

Search for...

Download Full Issue

Atrial Glutathione Content, Calcium Current, and Contractility*

Cynthia A. Carnes • Paul M.L. Janssen • Mary L. Ruehr • ... A. Marc Gillinov • Robert L. Hamlin •

David R. Van Wagoner ⚲ ✉ • Show all authors • Show footnotes

PlumX Metrics

Atrial fibrillation (AF) is characterized by decreased L-type calcium current ($I_{Ca,L}$) in atrial myocytes and decreased atrial contractility. Oxidant stress and redox modulation of calcium channels are implicated in these pathologic changes. We evaluated the relationship between glutathione content (the primary cellular reducing moiety) and $I_{Ca,L}$ in atrial specimens from AF patients undergoing cardiac surgery. Left atrial glutathione content was significantly lower in patients with either paroxysmal or persistent AF relative to control patients with no history of AF. Incubation of atrial myocytes from AF patients (but not controls) with the glutathione precursor N-acetylcysteine caused a marked increase in $I_{Ca,L}$. To test the hypothesis that glutathione levels were mechanistically linked with the reduction in $I_{Ca,L}$, dogs were treated for 48 h with buthionine sulfoximine, an inhibitor of glutathione synthesis. Buthionine sulfoximine treatment resulted in a 24% reduction in canine atrial glutathione content, a reduction in atrial contractility, and an attenuation of $I_{Ca,L}$ in the canine atrial myocytes. Incubation of these myocytes with exogenous glutathione also restored $I_{Ca,L}$ to normal or greater than normal levels. To probe the mechanism linking decreased glutathione levels to down-regulation of I_{Ca}, the biotin switch technique was used to evaluate S-nitrosylation of calcium channels. S-Nitrosylation was apparent in left atrial tissues from AF patients; the extent of S-...lation was inversely related to tissue glutathione content. S-Nitrosylation was al.. ...ect...
...cells expressing recombinant human cardiac calcium channel subunits followir...

os

nitrosoglutathione. *S*-Nitrosylation may contribute to the glutathione-sensitive attenuation of $I_{Ca,L}$ observed in AF.

Atrial fibrillation (AF)[2] is characterized by rapid electrical activation of the atria. Persistent AF results in phenotypic electrical and structural remodeling of the atria. Calcium influx via I_{Ca} triggers calcium release from intracellular stores and is an essential first step in excitation-contraction coupling and a critical determinant of atrial contractility. In atrial myocytes from patients with persistent AF ([1]) or from animals with pacing-induced AF ([2]), calcium current density is significantly decreased. The time course of contractile impairment following the onset of AF ([3]) or rapid atrial pacing ([4]) parallels the down-regulation of I_{Ca}, and contractile recovery proceeding cardioversion follows a time course similar to that of reverse electrical remodeling ([4]). Reports characterizing the impact of AF on the expression of the calcium channel pore subunit in human AF and in experimental models have had conflicting results ([5], [6]); the mechanisms by which $I_{Ca,L}$ down-regulation occurs are not fully resolved.

In a porcine model of rapid atrial pacing, superoxide production is increased ([7]), and nitric oxide production is decreased ([8]). Oxidant-generating pathways can shift the myocyte intracellular redox environment from its normally reduced state to a more oxidized one. A shift in oxidation state has been implicated in early atrial electrical remodeling in a canine rapid atrial pacing model of AF ([9]) and in the remodeling accompanying persistent AF ([10]). In addition to I_{Ca} ([11]), the ryanodine receptor, RyR2, and the transient outward K^+ current, I_{to}, are also redox-sensitive ([12], [13]). Each of these currents modulates the atrial action potential and atrial contractility.

Phosphorylation is the signaling pathway most commonly associated with modulation of calcium channel activity. Oxidant generation and redox changes are important elements in the β-adrenergic regulation of I_{Ca} ([14]), and altered calcium channel phosphorylation has been shown to contribute to the decrement in calcium channel activity during AF ([15]). However, intracellular redox state can modulate protein function by several additional pathways. Redox state directly regulates the conformation and activity of proteins. Redox-dependent posttranslational modifications of proteins include nitration of tyrosine residues and *S*-nitrosylation of cysteine residues, among others. Nitration involves the interaction of peroxynitrite anion or another reactive nitrogen species with protein tyrosine residues and is generally indicative of oxidative damage ([16]). *S*-Nitrosylation involves the reversible transfer of NO to a cysteine residue of an acceptor protein and   ee considered cytoprotective ([17]). Two proteins essential for cardiac excitation-contractio   ⟨   ɔlir   ⟩

the ryanodine receptor ([18]) and the L-type Ca^{2+} channel ([19]), have been shown to be nitrosylated. It is intriguing that mice conditionally overexpressing neuronal nitric-oxide synthase have lower I_{Ca} densities and contractility than do the wild type controls ([20]).

Disease states, including diabetes ([16]), hypertension ([21]), and heart failure ([22]), all common co-morbidities with AF, are characterized by evidence of increased oxidative stress. Under stressed conditions, cellular and plasma glutathione is oxidized, and cellular glutathione stores become depleted. Glutathione is the most abundant endogenous reducing agent and a critical modulator of cellular redox state. Since glutathione can act as an intracellular NO acceptor, alterations in the level of total cellular glutathione may have important consequences for both the redox-dependent and the NO-dependent regulation of ion channel activity.

Studies done in one of our laboratories ([1]) and others ([15], [23], [24]) have shown that I_{Ca} is decreased in atrial myocytes isolated from AF patients. Several years ago, we postulated that changes to the intracellular redox environment of myocytes from the fibrillating atria may contribute to the observed loss of calcium current ([25]). Here we have evaluated the redox- and glutathione-dependent modulation of I_{Ca} in myocytes from patients undergoing cardiac surgery for chronic AF. Because glutathione is an endogenous reducing agent important in maintaining a reduced intracellular environment, we evaluated whether glutathione levels are reduced in AF. We have also tested the impact of pharmacologic depletion of atrial glutathione on atrial function in an *in vivo* canine model system. Because redox state modulates the activity of cellular kinases and phosphatases, we have examined the calcium current response to β-adrenergic stimulation and correlated this response with atrial glutathione content. Many cardiovascular diseases are characterized by glutathione depletion; in this setting, *S*-nitrosylation of several cellular targets has been reported to increase ([26]). Thus, we explored calcium channel *S*-nitrosylation as a potential mechanism that may couple altered glutathione levels with modulation of calcium channel activity and contractility in AF.

MATERIALS AND METHODS

Human Atrial Studies—Table 1 summarizes relevant clinical characteristics of the cardiac surgery patients from whom left atrial appendage specimens were obtained. Left atrial tissue was brought to the laboratory from the operating room within 5 min of excision. Part of the specimen (~300 mg) was used for myocyte isolation, whereas adjacent areas were snap frozen in liquid nitrogen and stored at -80 °C for assessment of glutathione and *S*-nitrosylation levels. All procedures were performed between 2001 and 2005 with informed consent and approval from the Cleveland Clinic Institutional Review Board.

TABLE 1 Demographic and clinical characteristics of patients in study

Group	Age	Male/Female	EF	LA	MR	TR
			%	cm		
Controls	35	Male	53	3.5	3-4+	1+
	48	Male	65	4.1	3+	tr
	56	Male	60	4.5	4+	1+
	56	Male	25	3.4	tr	tr
	67	Male	60	4	2-3+	1+
	76	Male	45	nl	tr	tr

Open table in a new tab

Myocyte Isolation—Myocytes were isolated from the left atrial appendage (human or canine) using a chunk dissociation technique, as previously described (1). Yields of canine atrial myocytes were in the range of 40-60% calcium-tolerant, rod-shaped, well striated myocytes. Yields of human myocytes were lower (20-40%). Myocytes were maintained at room temperature until use. To determine whether exogenous *N*-acetylcysteine (NAC; a glutathione precursor) or glutathione modulated I_{Ca}, preparations were divided following isolation, with half stored in an incubation b containing 10 mM NAC or glutathione, whereas the remaining cells were held in an inc on
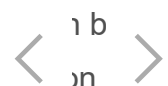
without additional antioxidant. The composition of this buffer was as follows: 118 mM NaCl, 25 mM NaHCO$_3$, 4.8 mM KCl, 1.2 mM MgCl$_2$, 1.2 mM KH$_2$PO$_4$, 10 mM taurine, 4 mM dextrose, 5 mM pyruvate, 2 mM mannitol, pH 7.4. Cells were incubated for a minimum of 1 h in NAC before recordings were initiated and for a minimum of 3 h in glutathione. Only myocytes with clear striations and sharp margins were used for the electrophysiological studies, and all measurements were made within 8 h of cell isolation.

Patch Clamp Experiments—Conventional whole cell patch clamp techniques were used. Data acquisition was performed with pClamp software (version 6.05+; Axon Instruments, Union City, CA) and an Axopatch (1C or 200A) patch clamp amplifier (Axon Instruments). The pipette solution contained 125 mM CsCl, 20 mM tetraethylammonium chloride, 5 mM MgATP, 3.6 mM creatine phosphate, 10 mM EGTA, 10 mM HEPES, pH 7.2. The bath solution (35 °C) contained 157 mM tetraethylammonium chloride, 1 mM CaCl$_2$, 0.5 mM MgCl$_2$, 10 mM HEPES, pH 7.4. I_{Ca} recordings began 3 min after patch rupture. Isoproterenol (1 µmol/liter) was used to test the response of I_{Ca} to maximal β-adrenergic receptor stimulation (steady state, ~4 min exposure). Electrophysiologic experiments were performed under continuous flow conditions at 35 ± 0.5 °C.

Canine Glutathione Depletion—L-Buthionine sulfoximine (BSO; Sigma) was dissolved in 30 ml of 0.9% NaCl immediately prior to intravenous administration. Young adult beagle hounds of either sex (5-12 kg) were randomly assigned to either active treatment (0.1 mmol/kg BSO, *n* = 10) or control dosing (30 ml of 0.9% NaCl injection, *n* = 10) twice daily for 2 days. On the morning of day 3, *in vivo* measurements were obtained prior to euthanasia and removal of the heart. All animal protocols were approved by the Institutional Animal Care and Use Committee of the Ohio State University.

In Vivo Physiologic Measurements—Dogs were lightly sedated for all conscious procedures (butorphanol, 0.1 mg/kg intramuscularly). Two-dimensional and M-mode echocardiography was performed at base line and daily thereafter (SSD 1400 (Aloka, Tokyo, Japan) with a 5 MHz transducer). Systolic blood pressure was measured in triplicate using an automated blood pressure device (Vet/BP model 6000; Sensor Devices Inc., Waukesha, WI). Electrocardiograms were recorded using a Biopac MP 100 (Biopac Systems, Santa Barbara, CA); lead I was used for P wave measurements. Electrocardiograms were digitized and stored for off-line analysis (acqKnowledge version 3.5, Biopac Systems, Santa Barbara, CA).

After induction of anesthesia with isoflorane, a bipolar electrode was advanced to the right atrium. Atrial effective refractory periods (ERPs) were determined at cycle lengths of 300, 250, and 200 ms, using a train of eight pacing stimuli at twice the diastolic pacing threshold, followed by an increasingly premature extrastimulus (5-ms decrement) delivered by a programmable atc

(Medtronic model 5325; Medtronic, Inc.). Inducibility of atrial arrhythmias was determined using a right atrial burst pacing protocol (10 Hz stimulation for 10 s). Inducibility was evaluated in triplicate at 5-min intervals.

In Vitro Physiology Studies: Contractility—In a separate set of experiments, dogs were randomized to treatment with BSO or vehicle control as above ($n = 3$ per group). Dissection and experimental procedures for trabeculae were as previously described (27). Briefly, using a stereomicroscope, ultrathin trabeculae were dissected from the right atria ($n = 20$ trabeculae) in a Krebs-Henseleit solution, containing 120 mmol/liter NaCl, 5.0 mmol/liter KCl, 2.0 mmol/liter $MgSO_4$, 1.2 mmol/liter NaH_2PO_4, 20 mmol/liter $NaHCO_3$, 0.25 mmol/liter $CaCl_2$, and 20 mmol/liter 2,3-butanedione monoxime in continuous equilibrium with 95% O_2, 5%CO_2. Only very small muscles (averages 237 ± 24 µm wide, 162 ± 17 µm thick, and 2.97 ± 0.32 mm long) were used. Muscles were mounted between a force transducer and a length displacement device, in the same solution (with omission of 2,3-butanedione monoxime and $CaCl_2$ increased to 1.5 mmol/liter). At 37 °C, stimulation at 1 Hz (20% above threshold) was initiated. After equilibration at optimal length, a force-frequency protocol was performed. Trabeculae were stimulated at frequencies of 1-5 Hz, and data were collected at steady state for each frequency. Next, the response to isoproterenol (1 nmol/liter to 1 µmol/liter) was assessed. Data were collected and analyzed with custom programs written in Labview.

Glutathione Assay—Atrial glutathione levels were measured using colorimetric assays (Oxis Research and Northwest Life Sciences). Intra-assay coefficient of variation was estimated as 0.6%, and interassay coefficient of variation was estimated as 3%. Frozen (-80 °C) tissue specimens, 20-60 mg each, were homogenized in vendor-recommended buffers for measurement of tissue glutathione.

S-Nitrosylation Measurement—The biotin switch technique (28) was used to assess the extent of nitrosylation of human LAA tissue or HEK cell lysates from cells stably overexpressing the α_{1C} subunit of the cardiac L-type Ca^{2+} channel (29). This technique labels nitrosylated cysteines with biotin, so that this posttranslational modification can be visualized. Briefly, left atrial appendage tissue or cells were homogenized in HEN buffer (250 mM Hepes-NaOH, 1 mM EDTA, 0.1 mM neocuproine). Free thiol groups were blocked with 20 mM methyl methane-thiosulfonate in HEN buffer with 1% SDS for 20 min at 50 °C. Free methyl methane-thiosulfonate was removed by acetone precipitation at -20 °C for 20 min. After centrifugation at 2000 × g for 10 min at 4 °C, the resulting pellet was resuspended in HEN buffer with 1% SDS. SNO groups were reduced with sodium ascorbate (1 mM), and free thiols were labeled with *N*-[6-(biotinamido)hexyl]-3′-(2′-pyridyldithio)-propionamide (4 mM; Pierce) for 1 h at 25 °C. All steps up to this point were rfc with minimal light at 4 °C to prevent the loss of endogenous *S*-nitrosylation. Following

labeling, a 20-µl aliquot was removed from each sample and added to 2× sample buffer. The sample was subjected to SDS-PAGE under nondenaturing conditions, and Western blot analysis was performed using a mouse anti-biotin antibody (Sigma) to label biotinylated, and thus nitrosylated, residues. The remainder of some samples was immunoprecipitated with a polyclonal antibody to the α_{1C} subunit of the L-type Ca^{2+} channel (Santa Cruz Biotechnology, Inc., Santa Cruz, CA), and immunoprecipitated protein was analyzed by Western blot analysis using an antibiotin antibody to determine the level of nitrosylation of the α_{1C} subunit.

Generation of Antibodies—Antibodies to the cardiac α_{1C} subunit (Fig. 6) were raised against synthetic peptides as described for the 2-3 loop antibody in Ref. 5. Further antigenic epitopes comprised the long N-terminal (KGTLVHEAQLN) and the α/β interaction domain in the 1-2 loop (KQQLEEDLKGYLKG) of the cardiac α_{1C} (Swiss-Prot accession number P15381). The antibodies were affinity-purified on respective peptide antigen columns.

FIGURE 6 *S*-**Nitrosylation of the α_{1C} subunit of the L-type calcium channel is increased in human AF tissue.** *A*, representative anti-biotin Western blot analysis (*WB*) of biotin-labeled *S*-nitrosylated residues showing three human tissue samples from control patients and three samples from patients with AF. *B*, the same blot was stripped and reprobed with antibodies to the 2-3 loop and N terminus of the α_{1C} subunit of the L-type calcium channel. Lower detection of the ~214-kDa band in the AF samples may reflect masking of the epitope by residual anti-biotin antibody. *C*, this composite image is an overlay of the biotinylated blot *A* (*red*) and the α_{1C} antibody staining (*B, black*). *D*, a blot from a separate gel run at the same time as the one in *A-C*, loaded with the same samples, probed with the same anti-α_{1C} antibodies used in *B* but not probed with the anti-biotin antibody. *E*, atrial tissue lysate was immunoprecipitated (*IP*) with an α_{1C} subunit-specific antibody, and then Western blot analysis was performed using an anti-biotin antibody. As a control, an unlabeled aliquot of the AF sample was immunoprecipitated with an α_{1C} subunit-specific antibody, and then Western blot analysis was performed using an anti-biotin antibody. In addition, a biotin-labeled aliquot of the AF sample was immunoprecipitated with rabbit serum, and then Western blot analysis was performed using an anti-biotin antibody. The *arrow* points to the α_{1C} subunit band. *F*, homogenates from HEK cells expressing the α_{1C} subunit of the L-type calcium channel were treated with 100 µmol/liter *S*-nitrosoglutathione (*GSNO*) for 20 min and subjected to the biotin switch technique. Lysate from these cells was immunoprecipitated with an α_{1C} subunit-specific antibody, and then Western blot analysis was performed using an anti-biotin antibody. *G*, summary densitometric analysis of mean relative band density of *S*-nitrosylated α_{1C} subunit of the L-type calcium channel. *, $p < 0.05$ compared with controls. *H, S*-nitrosylation of the α_{1C} subunit of the L-type calcium channel is

inversely related to the atrial glutathione content. The *line* represents a best linear fit of the relationship for all samples (r =-0.70, p = 0.025).

Reagents—Reagents, all analytical grade or higher, were purchased from Sigma, unless otherwise noted.

Statistical Analysis—Statistical analysis was performed using either Student's *t* test or analysis of variance, as appropriate. Statistical significance was defined as $p < 0.05$. Data are reported as mean ± S.E.

RESULTS

Glutathione Content Is Decreased in LAA Tissues from AF Patients and BSO-treated Dogs—Total glutathione content was evaluated in left atrial tissues from cardiac surgery patients with no history of AF and compared with that of persistent AF patients or patients with a history of paroxysmal AF but in normal sinus rhythm at the time of surgery (Table 1). Fig. 1A shows that relative to control patients with no history of AF, left atrial glutathione content was 65% lower in patients with persistent AF. Tissue from patients with a history of paroxysmal AF but in sinus rhythm at the time of surgery had glutathione levels 45% lower than controls, a value intermediate between that of controls and those in AF at surgery. Analysis of variance revealed that differences between groups were highly significant ($p < 0.001$).

FIGURE 1 Left atrial glutathione levels are decreased in human AF and in BSO-treated dogs. *A*, glutathione levels are plotted for human LAA tissues from control patients with no history of AF, from persistent AF patients in AF at surgery, and from paroxysmal AF patients in normal sinus rhythm at the time of surgery. Glutathione content was lower in both AF groups relative to controls (*, $p < 0.01$); glutathione levels were also lower in patients with persistent AF than in those from patients with paroxysmal AF but in normal sinus rhythm at surgery (*HxAF/SR*;‡, $p < 0.05$). *B*, total glutathione levels were decreased relative to controls in canine atrial tissue excised from BSO-treated dogs (*, $p < 0.02$). The number of tissue samples evaluated is indicated *within* each *bar*.

Fig. 1B shows the left atrial glutathione content in dogs treated for 48 h with or without BSO. Glutathione levels were lower (23.7%, $p < 0.02$) in atrial tissues from dogs treated for 48 h with BSO than in control animals (0.74 ± 0.06 *versus* 0.97 ± 0.06 µmol/g) (Fig. 1B).

Influence of NAC on Human Atrial Calcium Currents (ICa)—I_{Ca} was recorded from left atrial myocytes isolated from AF patients in AF at the time of surgery (Fig. 2). As described under "Materials and Methods," half of the myocytes from each preparation were stored in a buffer supplemented with 10 mmol/liter NAC, a glutathione precursor. Recordings were obtained under base line conditions and following exposure to isoproterenol (4-min exposure, 1 µM) (Fig. 2, A-D). NAC exposure significantly increased human atrial I_{Ca} in myocytes from AF patients. Base line I_{Ca} was ~70% higher in the myocytes preincubated with NAC relative to those not similarly incubated with NAC (-11.85 ± 1.4 pA/pF *versus* -6.97 ± 0.9 pA/pF, $p < 0.002$). Current-voltage relations for the responses to NAC incubation and to isoproterenol stimulation are summarized in Fig. 2E. Although both isoproterenol and NAC increased I_{Ca}, the leftward shift in the current-voltage relations typically observed following adrenergic stimulation were not present following NAC exposure alone. Peak I_{Ca} densities for each group before and after isoproterenol stimulation are summarized and compared in Fig. 2F. Perhaps because of the up-regulation of basal I_{Ca}, the relative response of NAC-treated myocytes to isoproterenol was attenuated relative to that of myocytes not treated with NAC (Fig. 2F). These results suggest that NAC and isoproterenol have discrete effects on the calcium channel. Interestingly, in myocytes from two patients with no history of AF, incubation with 10 mM NAC had no significant effect on peak I_{Ca} (-9.0 ± 2.6 pA/pF ($n = 3$) in control bath, *versus* -11.1 ± 0.7 pA/pF ($n = 3$) in NAC, $p = 0.68$).

Figure thumbnail gr2

FIGURE 2 ***N*-Acetylcysteine incubation increases** I_{Ca} **in human AF.** *A*, voltage-clamp protocol. Myocytes were held at -60 mV and stepped to potentials from -40 to +30 mV in 10-mV increments. *B-E*, representative control I_{Ca} traces from a human AF myocyte maintained in a control incubation buffer (*B*), before and after superfusion with 1 µM isoproterenol (*C*). Shown are similar recordings from a different myocyte incubated (>1 h) in a buffer supplemented with 10 mmol/liter *N*-acetylcysteine prior to recording (*D*) and following superfusion with 1µM isoproterenol (*E*). Current densities are normalized to cell capacitance (pA/pF). *F*, current-voltage relations for all myocyte groups studied. The number of myocytes in each group is shown in the legend (6-10 patients/group). *G*, summary plot comparison of paired peak I_{Ca} data (b   nd ⟨ ⟩

isoproterenol exposure) from myocytes isolated from human AF left atria and incubated in a control buffer or in one supplemented with 10 mmol/liter *N*-acetylcysteine. Statistical significance (unpaired *t* test) is indicated *above* the *bars*. Patients whose myocytes were evaluated in this study are indicated in Table 1.

View Large Image | Download Hi-res image | Download (PPT)

Effects of BSO on Canine Atrial Function, Muscle Contractility, and Calcium Currents—To more systematically evaluate the functional impact of glutathione depletion on atrial contractility and calcium currents, 10 dogs were treated with BSO (a γ-glutamyl synthetase inhibitor) for 48 h prior to echocardiographic examination of cardiac function and *ex vivo* electrophysiologic and contractile characterization and compared with the same number of control (untreated) animals.

In Vivo Effects of BSO—As summarized in Table 2, there were no base line differences between groups with respect to resting heart rate, P wave duration, left atrial diameter, left atrial contractility, left ventricular fractional shortening, or peak A wave velocity. The only significant difference between groups prior to initiation of treatment was a slightly higher systolic blood pressure in the BSO-treated dogs. There was no significant difference in systolic blood pressure or heart rate between groups after 48 h of treatment. In addition, atrial conduction (assessed by P wave duration) was unchanged from base line in either treatment group. Echocardiography revealed no significant changes in left ventricular internal diameter-diastole, left ventricular internal diameter-systole, left ventricular fractional shortening, peak E wave velocity, or left atrial diameters or areas in either group. However, peak A wave velocity, a measure of atrial function, was reduced an average of 24.3% in the BSO-treated dogs from 39.6 ± 3.2 to 28.3 ± 2.18 m/s (Fig. 3A, paired *t* test, $p < 0.007$).

TABLE 2 Canine base line (pretreatment) *in vivo* cardiovascular function (means ± S.E.)

Group	SBP	HR	P wave duration	LV FS	Peak A wave velocity
	mm Hg	bpm	ms	%	m/s
Control (n = 10)	127 ± 3	92 ± 21	40.3 ± 1.4	42.2 ± 1.8	40.3 ± 2.3
BSO, 0.2 mmol/kg/day (n = 10)	140 ± 4[a]	111 ± 20	39.9 ± 1.4	41.5 ± 1.3	39.7 ± 3.2

a p = 0.025.

Open table in a new tab

Figure thumbnail gr3

FIGURE 3 **BSO treatment abbreviates atrial ERP and decreases contractility in a rate-dependent manner.** *A*, summary of echocardiographic measurements shows that A wave velocity (reflecting synchronized atrial contractile activity, measured during spontaneous sinus rhythm) was significantly reduced in BSO-treated dogs ($p < 0.007$). *B*, the atrial effective refractory period was significantly reduced in dogs treated with BSO ($p < 0.001$). *Open bars*, control group; *shaded bars*, BSO-treated group. *, a significant difference between treatment groups at a specific cycle length ($p < 0.05$). *C*, force-frequency response of active tension development by isolated atrial trabeculae from BSO-treated dogs is impaired compared with controls at all stimulus rates above 1 Hz ($p < 0.05$).

View Large Image | Download Hi-res image | Download (PPT)

Atrial ERPs were assessed at cycle lengths of 300, 250, and 200 ms prior to euthanasia. Analysis of variance from studies at all rates revealed that BSO treatment significantly shortened ERPs compared with the control group ($p < 0.001$). Abbreviation of the ERP by BSO treatment was greatest at the highest stimulation rates (Fig. 3B). There was no difference in either inducibility or duration of atrial arrhythmias between the two groups, with 2 of 10 control and 2 of 10 BSO-treated dogs having brief (<5 s) inducible atrial fibrillation. One control dog experienced an episode of

<   >

induced atrial flutter lasting more than 5 min. No spontaneous arrhythmias were detected during routine, conscious electrocardiogram monitoring.

In Vitro Contractility: Effects of BSO—Contractility was further assessed by measuring the force-frequency response of isolated canine atrial trabeculae from control dogs or those pretreated with BSO. During 1-Hz stimulation, developed force was slightly decreased in BSO-treated dogs compared with control dogs (22.4 ± 1.7 mN/mm^2 *versus* 27.3 ± 4.1 mN/mm^2). This difference was more pronounced at higher frequencies (Fig. 3C). In controls, at 4 or 5 Hz, developed force increased by 76 or 70%, respectively. In BSO-treated animals, developed force *decreased* by 5% at 4 Hz and by 20% at 5 Hz. Time to peak tension increased significantly in trabeculae from BSO-treated animals (75.9 ± 1.3 *versus* 70.5 ± 1.2 ms, $p < 0.0001$). Time for relaxation to 50% was also prolonged in the BSO-treated animals (39.9 ± 1.2 *versus* 36.6 ± 1.1 ms, $p < 0.05$).

Effects of BSO on Canine Atrial Calcium Currents—I_{Ca} was measured in myocytes isolated from the atria of control or BSO-treated animals to correlate the decrease in force-frequency response in isolated atrial trabeculae with I_{Ca} changes in individual myocytes. Representative I_{Ca} traces are shown in Fig. 4. Peak I_{Ca} was significantly lower in canine atrial myocytes from BSO-treated animals ($p < 0.05$). Analysis of the relationship between I_{Ca} density and tissue glutathione content showed that I_{Ca} was inversely correlated with atrial glutathione concentration ($r^2 = -0.36$, $p = 0.05$; data not shown). BSO treatment had no effect on time-dependent recovery from inactivation or voltage dependence of steady-state inactivation.

Figure thumbnail gr4

FIGURE 4 **Modulation of canine left atrial I_{Ca} by exogenous glutathione.** Myocytes in *A-D* were of similar size, and currents were normalized to cell capacitance. Myocytes were held at -60 mV and stepped to potentials from -40 to +30 mV in 10-mV increments (as in Fig. 2). *A*, I_{Ca} recorded from a representative control canine myocyte. *B*, I_{Ca} from a canine myocyte following *in vivo* treatment with BSO. *C*, I_{Ca} from a control canine myocyte following incubation (>3 h) with 10 mmol/liter glutathione. *D*, I_{Ca} from a canine myocyte following *in vivo* BSO treatment and 10 mmol/liter glutathione incubation. *E*, summary data of peak I_{Ca} (mean ± S.E.). The number of observations is indicated in each *bar*. *, difference from control ($p < 0.05$); #, difference from BSO ($p < 0.05$).

View Large Image | Download Hi-res image | Download (PPT)

To further evaluate the role of glutathione depletion on I_{Ca}, experiments were performed in which myocytes were divided into two populations after isolation, with half incubated (>3h) in a solution containing 10 mmol/liter glutathione. Glutathione incubation increased I_{Ca} in myocytes from control and BSO-treated animals; however, the response to glutathione incubation was greater in the myocytes from the BSO-treated animals (Fig. 4, C and D). Following incubation with glutathione, there was no difference in peak I_{Ca} between myocytes from control and BSO-treated animals (Fig. 4E, $p = 0.24$).

Canine Atrial β-Adrenergic Responses—In myocytes from BSO-treated dogs, isoproterenol-stimulated I_{Ca} was significantly lower than in controls (Fig. 5A, $p < 0.05$). There was no significant difference in isoproterenol-stimulated I_{Ca} between control and BSO-treated myocytes after incubation with glutathione. Concordant with the I_{Ca} measurements, the contractile response to isoproterenol of BSO-treated atrial trabeculae was also significantly attenuated (representative *traces* in Fig. 5B). As summarized in Fig. 5C, the control group displayed a robust response, and at the highest concentration of isoproterenol (1 µmol/liter), active force in control preparations had risen from 23.3 ± 3.7 to 78.5 ± 8.9 mN/mm^2, representing an average individual increase of 315 ± 72%. After BSO treatment, at 1 µmol/liter isoproterenol, active force rose from 18.1 ± 1.7 to 36.6 ± 4.3 mN/mm^2 (113 ± 30%).

FIGURE 5 Electrophysiologic and contractile responses to β-adrenergic stimulation are attenuated after BSO treatment. *A*, mean peak I_{Ca} densities ± S.E. for isoproterenol-stimulated currents, with and without exogenous glutathione incubation. The number of observations is indicated *within* each bar.*, $p < 0.05$ compared with myocytes from control dogs. *B*, representative atrial trabecular tension transient, 1-Hz stimulation, from control and BSO-treated dogs, in the absence and presence of maximal (1 µM) β-adrenergic stimulation with isoproterenol. *C*, summary of tension data shows that the effect of isoproterenol on developed tension is reduced in trabeculae from BSO-treated dogs. *Squares*, control atria; *circles*, BSO-treated atria. *, $p < 0.05$ compared with controls.

View Large Image | Download Hi-res image | Download (PPT)

S-Nitrosylation of α1C Subunit of L-type Calcium Channel in Human AF Samples—Glutathione depletion has been associated with an increase in *S*-nitrosylation of protein thiols (26, 30), and *S*-nitrosylation of the calcium channel has been associated with a decrease in I_{ca} (19). We used the biotin switch technique to evaluate the extent of endogenous *S*-nitrosylation of protein   〈 e s 〉

control and AF samples used to assess glutathione levels. A biotin-labeled band representing a nitrosylated cysteine residue was detected around 214 kDa in samples from patients with a history of AF (Fig. 6A). Additional biotin-labeled bands were detected above 420 kDa, at 160 kDa, and at ~64 kDa. The apparent molecular mass of the band around 214 kDa is consistent with that of the α_{1C} subunit of the L-type calcium channel. Blots were reprobed with two antibodies to the α_{1C} subunit (Fig. 6B). An antibody specific for the 2-3 loop preferentially recognized a band greater than 247 kDa; an antibody specific for the N terminus of the α_{1C} subunit preferentially labeled a protein around 214 kDa. This band appeared in some of the control samples but was less readily detected in the AF samples (Fig. 6B). The composite image (Fig. 6C) shows that the band detected by the calcium channel N terminus antibody ran at the same position as the band representing the nitrosylated protein (Fig. 6A). Biotinylation and/or the anti-biotin antibody attenuated detection of the ~214 kDa band (Fig. 6B), since this band was evident in all specimens and of comparable density in each lane of a blot not probed for biotin (Fig. 6D). A very similar staining pattern was obtained with an antibody directed against the 1-2 loop of the α_{1C} (data not shown). Because density of the α_{1C} subunit was not increased in the samples from AF patients, increased nitrosylation intensity must reflect increased nitrosylation of the calcium channel. Densitometric analysis of the biotinylated Western blots showed that nitrosylation of the α_{1C} subunit in the AF samples was increased 4.85-fold in the AF *versus* control samples ($p < 0.03$; Fig. 6G).

Lysate from one of the samples that was biotin-labeled was immunoprecipitated with an antibody to the α_{1C} subunit and subjected to SDS-PAGE and Western blot analysis using an anti-biotin antibody to confirm that the immunoreactive band detected at ~214 kDa was the α_{1C} subunit. An immunoreactive band in the lane loaded with lysate was labeled with biotin and immunoprecipitated with an antibody to the α_{1C} subunit. No bands were detected in control lanes loaded with either lysate that had not been labeled with biotin or lysate that was immunoprecipitated with rabbit serum alone (Fig. 6E). To further confirm that the α_{1C} subunit of the human L-type calcium channel can be nitrosylated, HEK cells overexpressing the α_{1C} subunit were treated with the NO donor *S*-nitrosoglutathione (100 µmol/liter, 20 min) and subjected to the biotin switch technique in the same manner described for human atrial tissues. Lysate from these cells was immunoprecipitated with an antibody to the α_{1C} subunit, and then Western blot analysis was performed using a biotin primary antibody. In the presence of *S*-nitrosoglutathione, the α_{1C} subunit was nitrosylated (Fig. 6F).

To evaluate the relationship between tissue glutathione content and the extent of nitrosylation of the α_{1C} subunit, glutathione content was plotted against the density of immunoreactive bands detected on Western blots from the corresponding samples (Fig. 6H). Tissues with lower glutathione content

had more protein nitrosylation than tissues with greater glutathione content. This inverse correlation was significant ($p < 0.03$).

DISCUSSION

Redox state modulates numerous signaling pathways in normal and diseased tissues. Cardiac cells maintain a strongly reduced state via production and enzymatic regulation of glutathione, NADPH, and thioredoxin (31). Although transient changes in redox state play a physiological role in cell signaling (32), shifts toward a persistent oxidative state are associated with injury and aging (33, 34). Glutathione is the primary intracellular redox buffer. Diseases, including diabetes (35), obesity (36), and heart failure (37) are associated with glutathione depletion and evidence of systemic oxidative stress as well as increased risk of AF (38, 39, 40).

Acute loss of cardiac glutathione occurs during cardiac surgery; glutathione loss correlated with decreased ventricular function following surgery (41). Postoperative AF occurs in 20-40% of cardiac bypass surgery patients; advanced age and decreased atrial contractile function have been identified as predictors of postoperative AF (42). Here, atrial glutathione content was ~40% lower in left atrial samples from AF patients than in tissues from control patients with no history of AF (Fig. 1A), consistent with an AF-related increase in atrial oxidative stress (10) and decreased atrial contractile function (3). Increased wall stress leads to increased oxidant production (43, 44); valvular dysfunction (increasing atrial pressures and wall stress) in AF patients may contribute to the greater loss of glutathione in these patients. Risk factors, including diabetes, obesity, and age, are also relevant.

Calcium cycling is essential for contraction, and Ca^{2+} influx via the L-type calcium channel (I_{Ca}) is a critical determinant of contractility. A decrement in atrial myocyte I_{Ca} has been noted both in AF induced by rapid atrial pacing (2, 45, 46) and in studies of human atrial myocytes isolated from patients with AF (1, 23, 24). There is less agreement about the molecular basis for the down-regulation of I_{Ca}. Although several animal studies suggest transcriptional regulation as a primary mechanism for this response (6, 45), no change in the expression of the primary pore-forming channel subunits was detected in human AF studies (5, 15). This apparent conflict may reflect subtle differences between the rapid atrial pacing models and clinical AF.

The human cardiac calcium channel is modulated by hypoxia and redox state (11). To test the hypothesis that redox modulation contributes to the loss of I_{Ca} in human AF, we evaluated the impact of incubating myocytes isolated from AF patients with NAC (a glutathione precu ‹ Fi ›

shows that this treatment resulted in a robust increase in I_{Ca} in myocytes isolated from these patients. Attempts to correlate I_{Ca} with tissue glutathione levels revealed a trend for the lowest current densities to be present in myocytes isolated from tissues with the lowest glutathione content. Incubation of myocytes with NAC led to a significant increase in I_{Ca} both in the absence and in the presence of β-adrenergic stimulation (Fig. 2). NAC incubation had little effect on I_{Ca} in myocytes isolated from two patients with no history of AF. Because of the very limited access to appropriate control cases, it is difficult to fully study this issue using human tissues.

To systematically evaluate the impact of lower glutathione levels on atrial I_{Ca} and contractile function, experiments were performed in which dogs were treated for 48 h with BSO, a γ-glutamyl synthetase inhibitor. BSO decreased atrial glutathione content by ~24%, less than the decrement in glutathione noted in human AF tissues (Fig. 1B). Although this is a modest reduction, echocardiography (Fig. 3A) revealed significantly depressed A wave velocity (which reflects atrial contractile function) in BSO-treated animals. Contractile remodeling in AF is strongly associated with electrical remodeling, and early in AF the time course of contractile remodeling parallels that of electrical remodeling (4). Fig. 3B shows that the atrial ERP was reduced at all cycle lengths studied in the BSO-treated dogs. Abbreviation of atrial ERP was closely correlated with loss of contractile force generation in atrial trabeculae isolated from the BSO-treated dogs and a shift in the force-frequency response from a positive slope to a flat or negative slope (Fig. 3C).

Abbreviation of atrial ERP is consistent with a loss of I_{Ca} (2). I_{Ca} was decreased in canine atrial myocytes isolated from BSO-treated relative to untreated control animals (Fig. 4). The increased density of I_{Ca} of human atrial myocytes following incubation with NAC was paralleled by the response of canine atrial myocytes to glutathione incubation. This response was noted in myocytes isolated from both control and BSO-treated animals. It is notable that atrial glutathione levels in the control dogs were lower than the glutathione levels in control patients (Fig. 1).

In the presence of exogenous glutathione, canine atrial I_{Ca} from the BSO-treated animals was still lower than that recorded from the control animals. Altered calcium channel phosphorylation may contribute to the decrement in I_{Ca} in human AF (15). In the presence of isoproterenol (Fig. 5A), atrial I_{Ca} remained depressed in myocytes isolated from BSO-treated animals. Attenuation of I_{Ca} in treated myocytes in the presence of isoproterenol was paralleled by a diminished contractile response to isoproterenol in isolated atrial trabeculae (Fig. 5, B and C). Following incubation of myocytes from BSO-treated dogs with exogenous glutathione, the isoproterenol-stimulated calcium current density was essentially identical in both groups. Redox-dependent modulation of kinase (48) and/or phosphatase (49) activity may also contribute to the loss of I_{Ca} and contractile r   ıse the BSO-treated animals and, we speculate, in human AF. Although BSO treatment at   ed

I_{Ca} and contractility, it did not promote AF. Additional factors (dispersion of repolarization, altered excitability, neural influences, etc.) must also be necessary to promote arrhythmogenesis.

Although we did not evaluate the influence of glutathione or NAC treatment on atrial L-type calcium channel phosphorylation, we did investigate another form of redox-sensitive intracellular signaling. Reactive oxygen and nitrogen species can lead to posttranslational modifications of cellular proteins and alter bioactive lipids (50). It seems likely that posttranslational modification of channels has functional consequences. Oxidant stress is implicated in the modulation of calcium channels (49), sodium channels (51), and the ryanodine receptor (52). Experimental advances have made it possible to evaluate modification of protein thiols (53). Much like protein phosphorylation, the addition of an -NO group to a protein can dynamically modify its function. This type of regulation may provide a mechanism by which changes in oxidation state and NO metabolism dynamically modulate cell function. We found increased levels of nitrosylation in the human LAA samples with decreased levels of total glutathione and a history of AF (Fig. 6). In a similar manner, another study reported that glutathione depletion was associated with increased nitrosylation of mitochondrial proteins, and it was suggested that this posttranslational modification protected cells from irreversible protein oxidation (26).

Here we report that the α_{1C} subunit of the L-type Ca^{2+} channel is a protein that is often highly nitrosylated in LAA samples from AF patients and that nitrosylation was inversely related to atrial glutathione content. This subunit was recently identified as the predominant protein that is S-nitrosylated in female mice following ischemia-reperfusion injury (19). In that setting, nitrosylation was also associated with decreased I_{Ca} and was suggested to be cardioprotective by attenuating Ca^{2+} overload-induced cellular injury. Mice conditionally overexpressing nNOS (with increased NO production adjacent to the calcium channel) have lower I_{Ca} densities and contractility than do the wild type controls (20). Proteins in addition to the calcium channel also undergo nitrosylation (Fig. 6A). Ryanodine receptor nitrosylation is implicated abnormal regulation of calcium release and may contribute to spontaneous electrical activity (54).

AF is associated with both decreased I_{Ca} and evidence of increased oxidant production. As in ischemia-reperfusion injury, a down-regulation of I_{Ca} may be a short term response that protects myocytes from rate-induced calcium overload, preventing more extensive and irreversible proteolytic tissue injury (55). With adequate intracellular glutathione, this response may be mediated by S-nitrosylation of cysteine residues.

Integration of Results into a Coherent Model—These results may be integrated into a coherent framework. Under un-stressed conditions, intracellular redox state is maintained in a h ed

state. Under these conditions, available NO is most likely to interact with the abundant glutathione molecules within the myocyte. In the presence of ischemia-reperfusion, Ca^{2+} overload, or mitochondrial stress, production of intracellular oxidants is increased. Due to its abundance, these reactive species are likely to interact with glutathione, oxidizing it and releasing NO to interact with other target molecules (*e.g.* the calcium channel and ryanodine receptor). Nitrosylation of these targets may transiently decrease calcium influx and attenuate the energetic burden associated with calcium cycling. This generally cytoprotective effect may be associated with abbreviated ERP, decreased contractility, and increased risk of reentrant arrhythmia.

Under more persistent oxidant stress, oxidized glutathione may be exported from the cell faster than it is synthesized or recycled, leading to a state of net glutathione depletion. Aging is associated with decreased protection from oxidant injury (56), and aged hearts have lower glutathione levels (47). Under these conditions, intracellular oxidants may be more likely to interact with target proteins, leading to protein nitration (10) or other irreversible oxidation reactions (51). Analysis of tissue glutathione levels suggests that BSO-treated dogs and paroxysmal AF patients might be functionally comparable, whereas glutathione depletion may be greater in persistent AF.

Conclusions—Human AF is associated with oxidant stress and decreased atrial glutathione levels; persistent AF is associated with decreased atrial I_{Ca}. We propose that these observations are linked and that tissue glutathione acts to protect the myocyte from lethal oxidant injury. Glutathione levels also modulate the impact of other oxidants, including nitric oxide, on calcium channel activity. Calcium influx is at least transiently enhanced during the high rate activity of AF. Increased oxidant production during AF oxidizes glutathione, leading to a decrement in cellular glutathione levels. Glutathione levels also impact the adrenergic modulation of the calcium channel.

Although suppression of excessive oxidant production, prevention of ERP changes, and maintenance of atrial contractility appear to be desirable goals, a transient decrement in I_{Ca} may protect the atria from calcium overload-induced apoptosis and/or proteolysis. In this regard, oxidant-mediated changes may parallel the effects of β-adrenergic receptor antagonists, limiting calcium influx and force generation but improving prospects for long term survival.

Acknowledgments

References

1. Van Wagoner D.R. • Pond A.L. • Lamorgese M. • Rossie S.S. • McCarthy P.M. • Nerbonne J.M.
   Circ. Res. 1999; **85**: 428-436

   View in Article ∧

   Scopus (498) • PubMed • Crossref • Google Scholar

2. Yue L. • Feng J. • Gaspo R. • Li G.-R. • Wang Z. • Nattel S.
   Circ. Res. 1997; **81**: 512-525

   View in Article ∧

   Scopus (717) • PubMed • Crossref • Google Scholar

3. Schotten U. • Ausma J. • Stellbrink C. • Sabatschus I. • Vogel M. • Frechen D. • Schoendube F. • Hanrath P. • Allessie M.A.
   Circulation. 2001; **103**: 691-698

   View in Article ∧

   Scopus (230) • PubMed • Crossref • Google Scholar

4. Schotten U. • Duytschaever M. • Ausma J. • Eijsbouts S. • Neuberger H.R. • Allessie M.
   Circulation. 2003; **107**: 1433-1439

   View in Article ∧

   Scopus (138) • PubMed • Crossref • Google Scholar

5. Schotten U. • Haase H. • Frechen D. • Greiser M. • Stellbrink C. • Vazquez-Jimenez J.F. • Morano I. • Allessie M.A. • Hanrath P.
   J. Mol. Cell Cardiol. 2003; **35**: 437-443

View in Article ∧

Scopus (61) • PubMed • Abstract • Full Text • Full Text PDF • Google Scholar

6. Yue L. • Melnyk P. • Gaspo R. • Wang Z. • Nattel S.
    Circ. Res. 1999; **84**: 776-784

    View in Article ∧

    Scopus (317) • PubMed • Crossref • Google Scholar

7. Dudley S.C. • Hoch Jr., N.E. • McCann L.A. • Honeycutt C. • Diamandopoulos L. •
    Fukai T. • Harrison D.G. • Dikalov S.I. • Langberg J.
    Circulation. 2005; **112**: 1266-1273

    View in Article ∧

    Scopus (325) • PubMed • Crossref • Google Scholar

8. Cai H. • Li Z. • Goette A. • Mera F. • Honeycutt C. • Feterik K. • Wilcox J.N. •
    Dudley S.C. • Harrison Jr., D.G. • Langberg J.J.
    Circulation. 2002; **106**: 2854-2858

    View in Article ∧

    Scopus (326) • PubMed • Crossref • Google Scholar

9. Carnes C.A. • Chung M.K. • Nakayama T. • Nakayama H. • Baliga R.S. • Piao S. •
    Kanderian A. • Pavia S. • Hamlin R.L. • McCarthy P.M. • Bauer J.A. •
    Van Wagoner D.R.
    Circ. Res. 2001; **89**: 32e-38e

    View in Article ∧

    Scopus (461) • PubMed • Crossref • Google Scholar

10. Mihm M.J. • Yu F. • Carnes C.A. • Reiser P.J. • McCarthy P.M. • Van Wagoner D.R. •
    Bauer J.A.
    Circulation. 2001; **104**: 174-180

〈　〉

View in Article ∧

Scopus (599) • PubMed • Crossref • Google Scholar

11. Fearon I.M. • Palmer A.C. • Balmforth A.J. • Ball S.G. • Varadi G. • Peers C.

    J. Physiol. (Lond.). 1999; **514**: 629-637

    View in Article ∧

    Scopus (115) • Crossref • Google Scholar

12. Hidalgo C. • Donoso P. • Carrasco M.A.

    IUBMB Life. 2005; **57**: 315-322

    View in Article ∧

    Scopus (90) • PubMed • Crossref • Google Scholar

13. Xu Z. • Patel K.P. • Lou M.F. • Rozanski G.J.

    Cardiovasc. Res. 2002; **53**: 80-88

    View in Article ∧

    Scopus (72) • PubMed • Crossref • Google Scholar

14. Hool L.C. • Arthur P.G.

    Circ. Res. 2002; **91**: 601-609

    View in Article ∧

    Scopus (68) • PubMed • Crossref • Google Scholar

15. Christ T. • Boknik P. • Wohrl S. • Wettwer E. • Graf E.M. • Bosch R.F. • Knaut M. •
    Schmitz W. • Ravens U. • Dobrev D.

    Circulation. 2004; **110**: 2651-2657

    View in Article ∧

    Scopus (239) • PubMed • Crossref • Google Scholar

16. Pacher P. • Szabo C.

Curr. Opin. Pharmacol. 2006; **6**: 136-141

View in Article ∧

Scopus (155) • PubMed • Crossref • Google Scholar

17. Maejima Y. • Adachi S. • Morikawa K. • Ito H. • Isobe M.

J. Mol. Cell Cardiol. 2005; **38**: 163-174

View in Article ∧

Scopus (136) • PubMed • Abstract • Full Text • Full Text PDF • Google Scholar

18. Eu J.P. • Sun J. • Xu L. • Stamler J.S. • Meissner G.

Cell. 2000; **102**: 499-509

View in Article ∧

Scopus (387) • PubMed • Abstract • Full Text • Full Text PDF • Google Scholar

19. Sun J. • Picht E. • Ginsburg K.S. • Bers D.M. • Steenbergen C. • Murphy E.

Circ. Res. 2006; **98**: 403-411

View in Article ∧

Scopus (255) • PubMed • Crossref • Google Scholar

20. Burkard N. • Rokita A.G. • Kaufmann S.G. • Hallhuber M. • Wu R. • Hu K. • Hofmann U. • Bonz A. • Frantz S. • Cartwright E.J. • Neyses L. • Maier L.S. • Maier S.K. • Renne T. • Schuh K. • Ritter O.

Circ. Res. 2007; **100**: e32-e44

View in Article ∧

Scopus (86) • PubMed • Crossref • Google Scholar

21. Mueller C.F. • Widder J.D. • McNally J.S. • McCann L. • Jones D.P. • Harrison D.G.

Circ. Res. 2005; **97**: 637-644

View in Article ∧

Scopus (115) • PubMed • Crossref • Google Scholar

⟨ ⟩
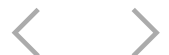
22. Giordano F.J.

    J. Clin. Invest. 2005; **115**: 500-508

    View in Article ∧

    Scopus (1252) • PubMed • Crossref • Google Scholar

23. Bosch R.F. • Zeng X. • Grammer J.B. • Popovic K. • Mewis C. • Kühlkamp V.

    Cardiovasc. Res. 1999; **44**: 121-131

    View in Article ∧

    Scopus (502) • PubMed • Crossref • Google Scholar

24. Skasa M. • Jungling E. • Picht E. • Schondube F. • Luckhoff A.

    Basic Res. Cardiol. 2001; **96**: 151-159

    View in Article ∧

    Scopus (68) • PubMed • Crossref • Google Scholar

25. Van Wagoner D.R.

    J. Cardiovasc. Electrophysiol. 2001; **12**: 183-184

    View in Article ∧

    Scopus (16) • PubMed • Crossref • Google Scholar

26. Whiteman M. • Chua Y.L. • Zhang D. • Duan W. • Liou Y.C. • Armstrong J.S.

    Biochem. Biophys. Res. Commun. 2006; **339**: 255-262

    View in Article ∧

    Scopus (36) • PubMed • Crossref • Google Scholar

27. Janssen P.M. • Lehnart S.E. • Prestle J. • Hasenfuss G.

    J. Mol. Cell Cardiol. 1999; **31**: 1419-1427

    View in Article ∧

    Scopus (46) • PubMed • Abstract • Full Text PDF • Google Scholar

⟨   ⟩

28. Jaffrey S.R. • Snyder S.H.

    Sci. STKE 2001. 2001; : L1

    View in Article ∧

    Google Scholar

29. Hudasek K. • Brown S.T. • Fearon I.M.

    Biochem. Biophys. Res. Commun. 2004; **318**: 135-141

    View in Article ∧

    Scopus (58) • PubMed • Crossref • Google Scholar

30. Han D. • Hanawa N. • Saberi B. • Kaplowitz N.

    Am. J. Physiol. 2006; **291**: G1-G7

    View in Article ∧

    Scopus (265) • PubMed • Crossref • Google Scholar

31. Li S. • Li X. • Rozanski G.J.

    J. Mol. Cell. Cardiol. 2003; **35**: 1145-1152

    View in Article ∧

    Scopus (55) • PubMed • Abstract • Full Text • Full Text PDF • Google Scholar

32. Liu H. • Colavitti R. • Rovira I.I. • Finkel T.

    Circ. Res. 2005; **97**: 967-974

    View in Article ∧

    Scopus (363) • PubMed • Crossref • Google Scholar

33. Cargnoni A. • Ceconi C. • Gaia G. • Agnoletti L. • Ferrari R.

    J. Mol. Cell. Cardiol. 2002; **34**: 997-1005

    View in Article ∧

    Scopus (29) • PubMed • Abstract • Full Text PDF • Google Scholar

‹ ›

34. Squier T.C. • Bigelow D.J.
Front. Biosci. 2000; **5**: D504-D526

    View in Article ∧

    PubMed • Crossref • Google Scholar

35. Martin-Gallan P. • Carrascosa A. • Gussinye M. • Dominguez C.
Free Radic. Biol. Med. 2003; **34**: 1563-1574

    View in Article ∧

    Scopus (329) • PubMed • Crossref • Google Scholar

36. Keaney J.F. • Larson Jr., M.G. • Vasan R.S. • Wilson P.W. • Lipinska I. • Corey D. •
Massaro J.M. • Sutherland P. • Vita J.A. • Benjamin E.J.
Arterioscler. Thromb. Vasc. Biol. 2003; **23**: 434-439

    View in Article ∧

    Scopus (1162) • PubMed • Crossref • Google Scholar

37. Adamy C. • Le Corvoisier P. • Candiani G. • Kirsch M. • Pavoine C. • Defer N. •
Bourin M.C. • Su J.B. • Vermes E. • Hittinger L. • Pecker E.
Arch. Mal Coeur Vaiss. 2005; **98**: 906-912

    View in Article ∧

    PubMed • Google Scholar

38. Benjamin E.J. • Levy D. • Vaziri S.M. • D'Agostino R.B. • Belanger A.J. • Wolf P.A.
J. Am. Med. Assoc. 1994; **271**: 840-844

    View in Article ∧

    Scopus (2751) • PubMed • Crossref • Google Scholar

39. Chung M.K. • Foldvary-Schaefer N. • Somers V.K. • Friedman P.A. • Wang P.J.
Nat. Clin. Pract. Cardiovasc. Med. 2004; **1**: 56-59

    View in Article ∧

⟨ ⟩

Scopus (16) • PubMed • Crossref • Google Scholar

40. Levy S.

Pacing Clin. Electrophysiol. 1997; **20**: 2670-2674

View in Article ∧

Scopus (72) • PubMed • Crossref • Google Scholar

41. De Vecchi E. • Pala M.G. • Di Credico G. • Agape V. • Paolini G. • Bonini P.A. • Grossi A. • Paroni R.

Heart. 1998; **79**: 242-247

View in Article ∧

Scopus (49) • PubMed • Crossref • Google Scholar

42. Leung J.M. • Bellows W.H. • Schiller N.B.

Eur. Heart J. 2004; **25**: 1836-1844

View in Article ∧

Scopus (34) • PubMed • Crossref • Google Scholar

43. Grote K. • Flach I. • Luchtefeld M. • Akin E. • Holland S.M. • Drexler H. • Schieffer B.

Circ. Res. 2003; **92**: e80-e86

View in Article ∧

PubMed • Crossref • Google Scholar

44. Takimoto E. • Champion H.C. • Li M. • Ren S. • Rodriguez E.R. • Tavazzi B. • Lazzarino G. • Paolocci N. • Gabrielson K.L. • Wang Y. • Kass D.A.

J. Clin. Invest. 2005; **115**: 1221-1231

View in Article ∧

Scopus (388) • PubMed • Crossref • Google Scholar

45. Bosch R.F. • Scherer C.R. • Rub N. • Wohrl S. • Steinmeyer K. • Haase H

Busch A.E. • Seipel L. • Kuhlkamp V.

J. Am. Coll. Cardiol. 2003; **41**: 858-869

View in Article ∧

Scopus (109) • PubMed • Crossref • Google Scholar

46. Yagi T. • Pu J. • Chandra P. • Hara M. • Danilo P. • Rosen Jr., M.R. • Boyden P.A.

Cardiovasc. Res. 2002; **54**: 405-415

View in Article ∧

Scopus (45) • PubMed • Crossref • Google Scholar

47. Stio M. • Iantomasi T. • Favilli F. • Marraccini P. • Lunghi B. • Vincenzini M.T. • Treves C.

Biochem. Cell Biol. 1994; **72**: 58-61

View in Article ∧

Scopus (47) • PubMed • Crossref • Google Scholar

48. Howe C.J. • Lahair M.M. • McCubrey J.A. • Franklin R.A.

J. Biol. Chem. 2004; **279**: 44573-44581

View in Article ∧

Scopus (115) • PubMed • Abstract • Full Text • Full Text PDF • Google Scholar

49. Campbell D.L. • Stamler J.S. • Strauss H.C.

J. Gen. Physiol. 1996; **108**: 277-293

View in Article ∧

Scopus (400) • PubMed • Crossref • Google Scholar

50. Fearon I.M.

Cardiovasc. Res. 2006; **69**: 855-864

View in Article ∧

Scopus (40) • PubMed • Crossref • Google Scholar

51. Fukuda K. • Davies S.S. • Nakajima T. • Ong B.H. • Kupershmidt S. • Fessel J. • Amarnath V. • Anderson M.E. • Boyden P.A. • Viswanathan P.C. • Roberts L.J. • Balser J.R.

    Circ. Res. 2005; **97**: 1262-1269

    View in Article ∧

    Scopus (114) • PubMed • Crossref • Google Scholar

52. Cheong E. • Tumbev V. • Stoyanovsky D. • Salama G.

    Cell Calcium. 2005; **38**: 481-488

    View in Article ∧

    Scopus (21) • PubMed • Crossref • Google Scholar

53. Jaffrey S.R. • Erdjument-Bromage H. • Ferris C.D. • Tempst P. • Snyder S.H.

    Nat. Cell Biol. 2001; **3**: 193-197

    View in Article ∧

    Scopus (1246) • PubMed • Crossref • Google Scholar

54. Salama G. • Menshikova E.V. • Abramson J.J.

    Antioxid. Redox. Signal. 2000; **2**: 5-16

    View in Article ∧

    Scopus (49) • PubMed • Crossref • Google Scholar

55. Brundel B.J. • Ausma J. • Van Gelder I.C. • Van der Want J.J. • Van Gilst W.H. • Crijns H.J. • Henning R.H.

    Cardiovasc. Res. 2002; **54**: 380-389

    View in Article ∧

    Scopus (126) • PubMed • Crossref • Google Scholar

56. Abete P. • Napoli C. • Santoro G. • Ferrara N. • Tritto I. • Chiariello M. • Rengo F. • Ambrosio G.

‹ ›

Article info

Publication history

Received: June 13, 2007

Identification

DOI: https://doi.org/10.1074/jbc.M704893200

Copyright

User license

ScienceDirect

Access this article on ScienceDirect

Figures
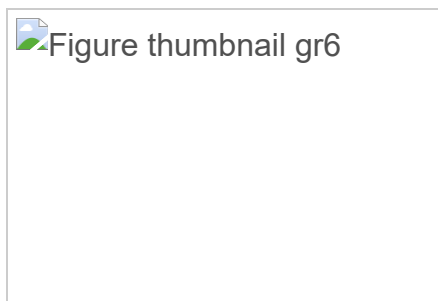
FIGURE 6 *S*-Nitrosylation…
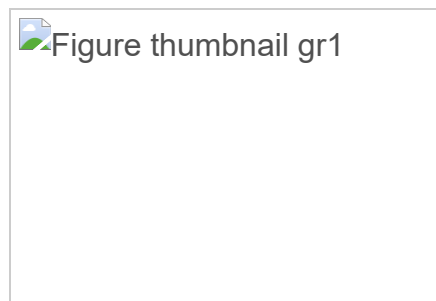
FIGURE 1 Left atrial gluta…
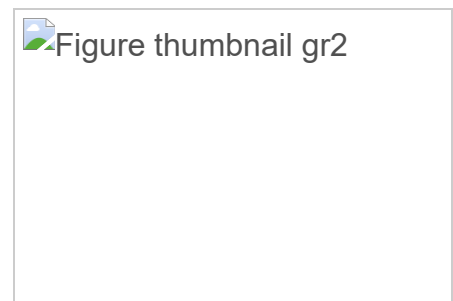
FIGURE 2 *N*-Acetylcystei…

‹ ›
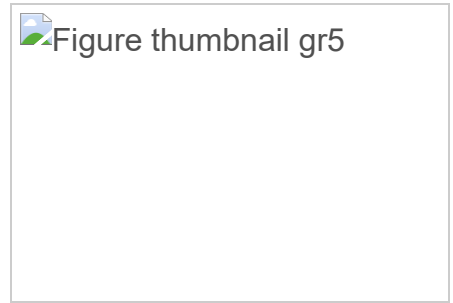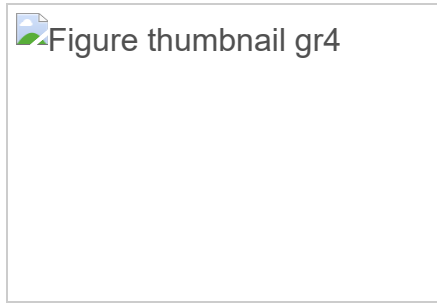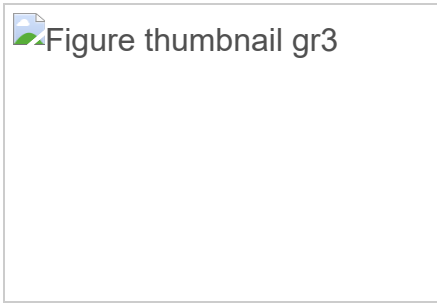
FIGURE 3 BSO treatment…

FIGURE 4 Modulation of …

FIGURE 5 Electrophysiol…

Tables

TABLE 1 : Demographic and clinical characteristics of patients in study

TABLE 2 : Canine base line (pretreatment) *in vivo* cardiovascular function (means ± S.E.)

Related Articles

ASBMB JOURNALS   JBC   JLR   MCP

ISSN 0021-9258

The content on this site is intended for healthcare professionals.

Privacy Policy   Terms and Conditions   Accessibility   Help & Contact

RELX™

‹   ›